Vol. 13(20), pp. 273-281, 30 December, 2018
DOI: 10.5897/IJPS2018.4759
Article Number: 734017459617
ISSN: 1992-1950

http://www.academicjournals.org/IJPS

International Journal of Physical Sciences

Full Length Research Paper

Magnetosphere convection electric field (MCEF) time variation from 1964 to 2009: Investigation on the signatures of the geoeffectiveness coronal mass ejections

Kaboré Salfo and Ouattara Frédéric*

Laboratoire de Recherche en Energétique et Météorologie de l'Espace (LAREME), Université Norbert Zongo (Anciennement Université de Koudougou), BP 376 Koudougou Burkina Faso.

Received 22 August, 2018; Accepted 27 November, 2018

The signatures of the geoeffectiveness solar disturbed events on the Magnetosphere Convection Electric Field (MCEF) universal time variation from 1964 to 2009 are investigated. Here, attention is focused our on the periods concerned by the whole shock activity and by the different types of the geoeffectiveness Coronal Mass Ejections (CMEs) which are one-day-shock, two-days-shock and three-days-shock. The investigation is made with respect to the orientation of the Interplanetary Magnetic Field (IMF). The MCEF time profiles show three different trends except for one-day-shock activity and for three-days-shock activity where we have four trends and one trend, respectively. The MCEF time profiles of the whole disturbed activity, the all shock activity and the one-day-shock activity present the initial phase where the Interplanetary Magnetic Field (IMF) is southward. During the two-days-shock activity, the initial phase of the MCEF shows a non-sensitive trend to the change of the direction of the IMF z-component while for the three-days-shock activity, the MCEF always exhibits the signature of the northward IMF. The last trend of the MCEF time profile shows the southward IMF signature except for the one-day-shock and the three-days-shock activities where that of the northward IMF was seen.

Key words: Magnetosphere convection electric field, interplanetary magnetic field, shock activity, coronal mass ejections (CMEs).

INTRODUCTION

The magnetosphere created by the solar wind is a very sensitive and dynamic entity (Russel, 1979) a behaviour that depends on the properties of the solar wind plasma and its frozen magnetic field (Mc Pherron et al., 2007). According to Mc Pherron et al. (2007), there are three possible magnetic topologies during the interaction between the solar wind and the planetary magnetosphere. Among them, we can cite the topology where a magnetic line might not intersect the Earth at all and that where a magnetic line might intersect the surface of the Earth

*Corresponding author. E-mail: fojals@yahoo.fr.

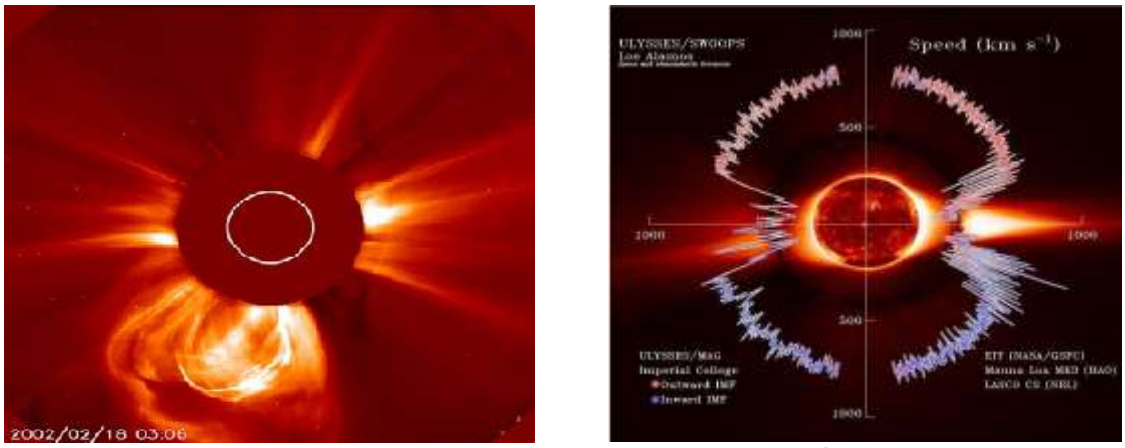

a b

Figure 1. Solar disturbance events. The panel a concerns high speed solar wind stream coming from coronal holes, slow solar wind stream coming from the neutral sheet and the CMEs. The panel b shows the two type of wind speed as measured by ULYSSE with the outward IMF (in red) and inward IMF (in blue).

twice (Russel, 2007). During the topology where there is an interaction between the solar wind and the planetary magnetosphere, two mechanisms are invoked to explain such interaction. The first one concerns the mechanism of Axford and Hines (1961), namely the viscous interaction (always present) where closed magnetic flux tubes are transported from the dayside to nightside. The second mechanism is that of Dungey (1961), namely magnetism reconnection. In that case, Russell (1979) notes that when the interplanetary magnetic field (IMF) is southward, its field lines convect along the solar wind break in half and join partners with magnetospheric lines and when the IMF is northward, the reconnection cannot take place at the nose of the magnetosphere but there are other places where antiparallel fields occur and it might take place.

It is known that there are two approaches to magnetospheric studies (Russel, 1979): (1) the statistical approach in which one thing is examined many times and (2) the case history approach in which one or two examples are looking very carefully. The present work concerns the first approach.

Several authors (Legrand and Simon, 1989; Richardson et al;, 2000; Richardson and Cane, 2002; Ouattara and Amory Mazaudier, 2009) showed that the geomagnetic storms [defined as global magnetic disturbances that result from the interaction between magnetized plasma propagating from the Sun and magnetic fields in the near-Earth space environment (Tommaso et al., 2016)] can be due to (1) recurrent activity (due to solar high stream wind coming from coronal holes), (2) shock activity (produced by the geoeffectiveness CMEs) and (3) fluctuating activity (caused by the geoeffectiveness fluctuating solar wind provoked by the fluctuation of solar neutral sheet) (Figure 1).

It is well known that the state of the Earth magnetosphere depends on the orientation of the IMF z-component (namely B_z and perpendicular to the ecliptic plan) during solar Wind-Earth magnetosphere interactions or CMEs-Earth magnetosphere interactions. Here we are concerned with the statistical behaviour of the Magnetosphere Convection Electric Field (MCEF) time variation (Universal Time: UT) under the action of the geoeffectiveness CMEs with respect to orientation of the IMF z-component. As shown by Gyébré et al. (2015), the shock activity due to the geoeffectiveness CMEs action can be divided into three types with respect to their time duration (one-day-shock, two-days-shock and the three-days-shock; detail on this typology is subsequently given as the present paper deals with each type of shock action on the Earth MCEF by taking into account the orientation of the IMF z-component.

For evaluating the different solar events impact on the Earth magnetosphere and specifically that of the three types of shock activity in the Earth MCEF, in our study we follow the method of Legrand and Simon (1989) that consists of using a pixel diagram for getting the overview of the yearly geoeffectiveness solar events; this overview can be extended to the whole period involved with given a continuum of several pixel diagrams. It is important to underline that this method does not require the knowledge of solar wind parameters for selecting each type of solar events (quiet or each type of disturbed events). This is in view of the fact that this method has been developing before having all solar wind parameters through satellites data (year 1989) and has been validated by Ouattara and Amory Mazaudier (2009). Therefore, pixel diagram appears as a good tool because its gives an excellent result during the evaluation of geomagnetic storms effects on ionosphere (e.g. Gyébré et al., 2018 and the reference therein about the use of the pixel diagrams). Thus, it is now clear that our objective is not to determine the different solar geoeffectiveness events by using the characteristic of the solar wind

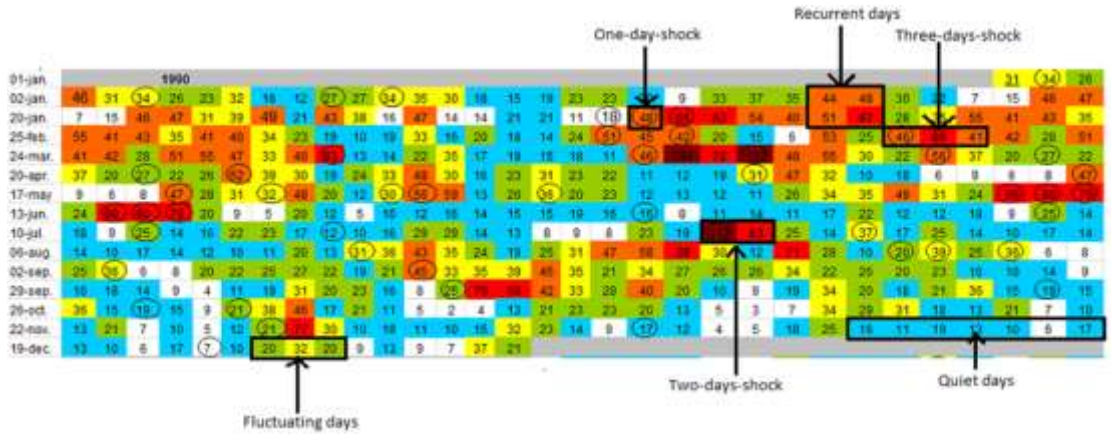

Figure 2. Pixel diagram of the year 1990 where are highlighted the four geomagnetic days with each type of shock activity.

parameters (that is already done by a pixel diagram) but to understand and to analyse each geoeffectiveness solar event (identifying by a pixel diagram) impact on the Earth's magnetosphere. This will be done with respect to the orientation of the IMF z-component.

In the present paper, we focus our attention on the impacts of the geoeffectiveness CMEs. The other geoeffectiveness disturbed events impacts will be analysed in our coming papers. The novelty of the present investigation is based on the consideration of the different types of shock activity.

Before analysing the Universal Time (UT) variability of the Earth MCEF (E_M) [that is, the electric field imposed on the magnetosphere by the solar wind interaction] under the shock conditions, we firstly analyse its UT variation during quiet periods and secondly during the whole disturbed periods (periods due to recurrent, fluctuating and shock activities) in order to appreciate the impact of the whole disturbed conditions on UT variation of the Earth MCEF with respect to that of the quiet time. After analysing the UT variation of the Earth MCEF under the shock conditions, we focus our attention on the UT variation of the Earth MCEF during each type of the shock activity.

MATERIALS AND METHODS

For studying the UT variation of the Earth MCEF under the shock activity, several parameters are used: (1) the Mayaud (1971, 1972) geomagnetic index aa, (2) the sudden storm commencement (SSC) dates and (3) the y-component (namely Ey) of the solar wind motion electric field (SWEF) and expressed by $E_y = V.B_z$ where V is solar wind velocity and B_z the interplanetary magnetic field intensity in the direction perpendicular to the ecliptic plane.

Method for determining the shock activity

The shock activity days are determined by means of the pixel diagrams (Figure 1) carried out by using the aa daily values (Ouattara and Amory Mazaudier, 2009). These diagrams highlight the repartition of the geomagnetic data as a function of the solar activity as described by solar rotation (27 days) (Ouattara and Amory Mazaudier, 2009; Gyébré et al., 2015). The four geomagnetic classes of activity [(1) quiet activity due to the slow solar wind, (2) recurrent activity caused by the high stream solar wind, (3) fluctuating activity provoked by the fluctuating solar wind and (4) shock activity that results from the action of the geoeffectiveness CMEs (Coronal Mass Ejections)] as defined by Legrand and Simon (1989), Simon and Legrand (1989), Richardson et al. (2000) and Richardson and Cane (2002). Gyébré et al. (2015) divided the shock activity into three types according to their time duration (one day, two days and three days): (1) one-day-shock, (2) two-days-shock and (3) three-days-shock activities. The one-day-shock corresponds to only a day when SSC occurs whatever its arrival time; the two-days-shock is shown by the SSC day with a day after this day (the concerning two days are the total days where this shock effects are seen) and the three-days-shock is identified by the SSC day with two days after this day (the involved three days are the total days where this shock effects are observed) (Gyébré et al., 2015, 2018). A pixel diagram (Figure 2) shows the three types of shock activity.

For the specific period, the whole pixel diagrams exhibit 323 shock-days with 168 days of one-day-shock, 105 days of two-days-shock and 50 days of three-days-shock (Gyébré et al., 2015).

Method for determining the magnetospheric convection electric field

Because our investigation period involved several years before the availability of the overall measurements of the solar wind parameters, the UT variation of the MCEF (E_M) will be computed by using the linear correlation between the hourly data of the SWEF (E_y) and that of the MCEF established by Revah and Bauer (1982) and given by the following equation: $E_M = 0.13\,E_y + 0.09$. In this equation, the correlation coefficient (r) value is 0.97. The hourly values of the SWEF are taken from OMNIWEB web site: *http://omniweb.gsfc.nasa.gov/form/dx1.html* whereas those of the MCEF are computed through the above equation and for the period 1964-2009 (this period corresponds to the four solar cycles involved). It is important to note that each hourly E_M value is computed by using the hourly arithmetic mean values of the E_y

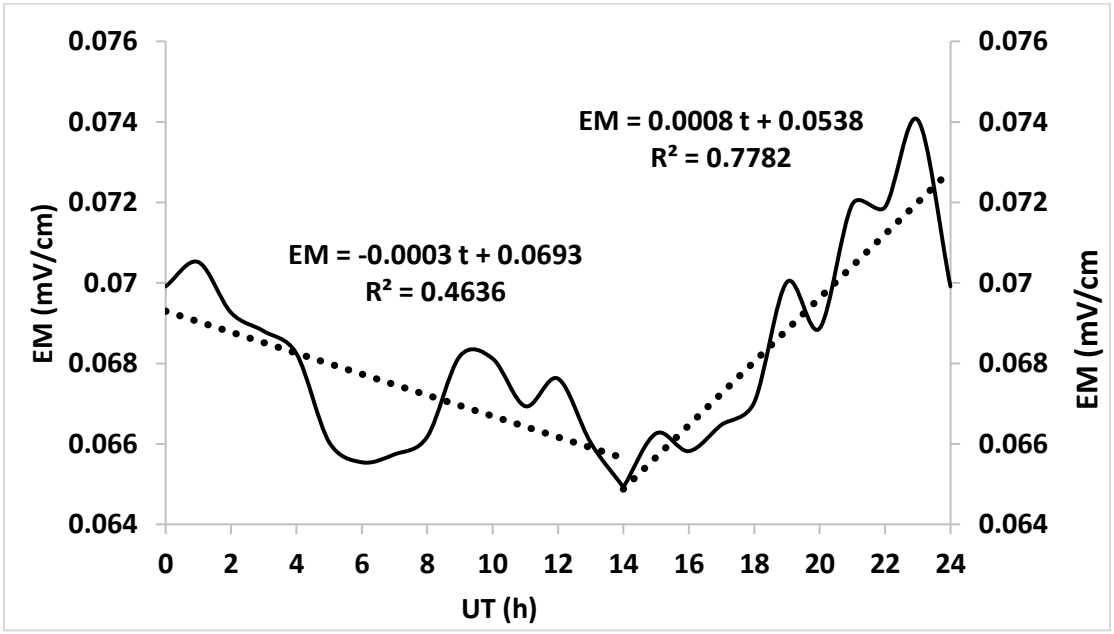

Figure 3. Magnetosphere convection electric field UT variation for quiet-days activity.

values of the concerning events for the period involved.

RESULTS AND DISCUSSION

Figure 3 shows the daytime variability of the MCEF during the quiet period. The linear curves are obtained by the least squares method. It can be seen that the MCEF graph highlights a decreasing phase from 0000 UT to 1400 UT and an increasing phase from 1400 UT to 24000 UT. The decreasing trend slope is $-\frac{3\ 10^{-4}mV}{cm.s}$ with correlation coefficient 0.609 and that of the increasing trend is $+\frac{8\ 10^{-4}mV}{cm.s}$ with correlation coefficient value 0.8822.

According to McPherron et al. (2007), a geomagnetically quiet time can be identified on one hand by the absence of the reconnection between the IMF and the geomagnetic field. During that case, tangential stress is applied by means of viscous interaction that transports closed magnetic flux tubes from the dayside to the night side (Axford and Hines, 1961); and on the other hand, by the reconnection between the northward IMF and the geomagnetic field. Croker (1992) noted that this reconnection connects in the tail lobes open lines to IMF lines and does not induce change in the amount of lobe flux. The analysis of the Figure 3 enable the assertion according to the model of Axford and Hines (1961) that the decreasing phase of the CMEF corresponds to the lack of closed magnetic flux tubes and its increasing phase pointed out the accumulation of the flux tubes by the viscous interaction. It may also be due to the reconnection in the tail lobes after the dayside reconnection between the geomagnetic field line and that of the northward IMF. The MCEF increases until the magnetosphere returns to a nominal condition characterized by its initial value. This is exhibited by the decreasing of the MCEF intensity from 2300 UT to 2400 UT.

The two different trends of the MCEF shows two different states of the magnetosphere: the first one characterized the period (0000 UT -1400 UT) of the viscous interaction where closed magnetic flux are transported tail ward and the second one corresponds to the period (1400 UT -2400 UT) of the reconnection in the tail lobes with the northward IMF. This result points out that 1400 UT is the time of the change of the state of the magnetosphere from viscous interaction and northward IMF interaction. The MCEF values oscillate between 0.0651 mV/cm (before 1400 UT) and 0.0426 mV/cm (after 1400 UT).

Figure 4 concerns the variability of the MCEF during the whole disturbed activity. One can see the increasing phase from 0000 UT to 1600 UT with increasing trend slope value of $\frac{3\ 10^{-4}mV}{cm.s}$ with 0.5857 as the correlation coefficient value and the decreasing phase from 1600 UT to 2100 UT with the decreasing slope value - $\frac{2.1\ 10^{-3}mV}{cm.s}$ with the correlation coefficient value of 0.9504. It appears as a night time increasing phase (from 2100 UT to 2400 UT) with $\frac{3.5\ 10^{-3}mV}{cm.s}$ as the trend slope value and the correlation coefficient value of 0.8557.

From 0000 UT to 1400 UT and from 1400 UT to 2100

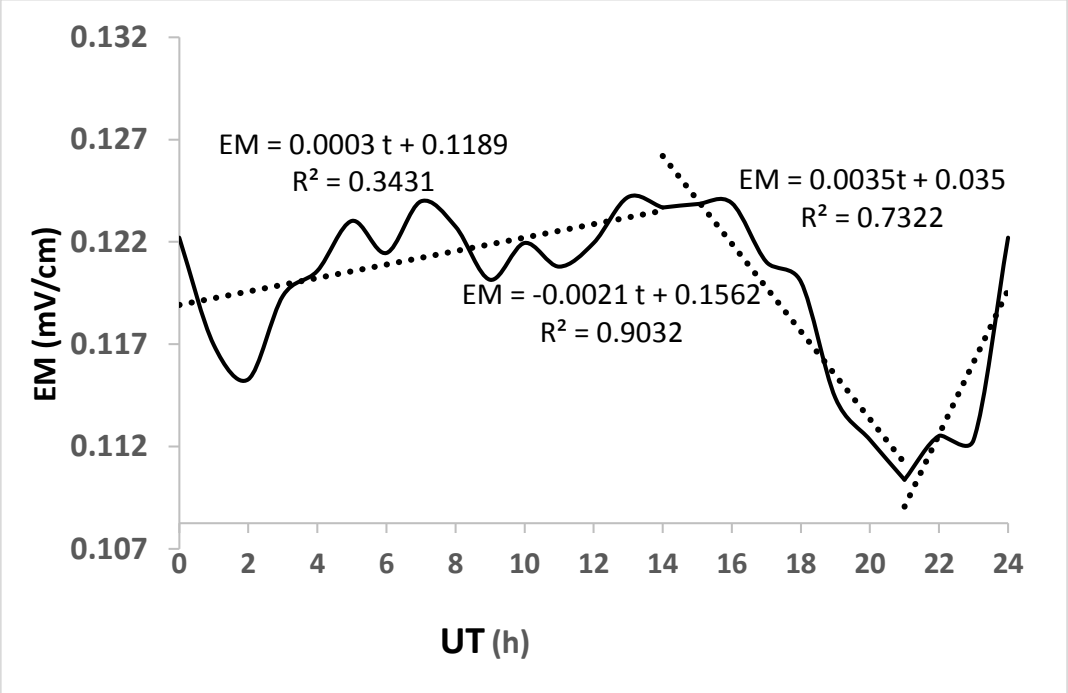

Figure 4. The same as Figure 3 but for the whole disturbed activity.

UT, the variability of MCEF for quiet time and that of disturbed period vary in opposite phase.

During disturbed time, the daily values of MCEF vary from 0.1100 to 0.1245 mV/cm with 0.1194 mV/cm as the daily mean value, while during quiet time, the MCEF varies from 0.06492 to 0.0720 mV/cm with daily mean value of 0.0676 mV/cm.

Figure 4 shows the time variation of MCEF during the geomagnetic storm conditions. In that case, there was a reconnection between the geomagnetic field line and that of the southward IMF (Dungey, 1961). It can be interpreted as the change of the IMF from northward (quiet condition) to southward (disturbed condition). Nishimura et al. (2009) noted that the MCEF reacts to this change and de Siqueira et al. (2011) underlines that the MCEF increases after the change of the IMF from northward to southward. Therefore, the increasing phase of the MCEF corresponds to the sustained southward IMF and consequently shows the storm main phase (Partamies et al., 2011). The beginning of this phase corresponds to the onset time of the change of the IMF from northward to southward. As this change implies the intensification of the ring current (Mannucci et al., 2008; Nishimura et al., 2009) and the geomagnetic storm is identified by the intensification of the ring current (Gonzalez et al., 1994), one can conclude that the increasing phase of the MCEF expressed the phase where geomagnetic activity increases. The decreasing phase which occurs after the increasing phase shows the phase of the change of the IMF from southward to northward. In fact, according to Kelley et al. (1979), the magnetospheric convection is weakened when the IMF turns from southward to northward. The following increasing phase may be due to the night side reconnection.

The analysis of the Figure 3 enables three phases: (1) the dayside reconnection with southward IMF, (2) the period (1600 UT -2100 UT) where the IMF changes from southward to northward and maintains northward until 2100 UT, and (3) the night side reconnection.

Figure 4 is devoted to the time variation of MCEF for the overall shock activity. The MCEF increases from 0000 UT to 1200 UT with the slope value of $\frac{2.3\ 10^{-3}mV}{cm.s}$ and 0.7115 as the correlation coefficient value. Between 1200 UT to 1500 UT, the MCEF decreases with - $\frac{2.27\ 10^{-2}mV}{cm.s}$ as its trend slope value with the correlation coefficient value of 0.9949. After 1500 UT until 2400 UT, we observe an increasing phase with $\frac{6.6\ 10^{-3}mV}{cm.s}$ as the trend slope and the correlation coefficient value of 0.8642.

When the MCEF acts, the overall shock activity varies from the minimum value of 0.137 mV/cm and the maximum value of 0.217 mV/cm with a mean value of 0.183 mV/cm.

In this case, the geomagnetic activities are considered due to the geoeffectiveness coronal mass ejections (CMEs). Figure 5 graph shows the same time variation as that of the Figure 4 except that the former (first and second) phases of the overall shock activity are shorter than that of the whole disturbed activity.

It can be retained from this figure that there are three

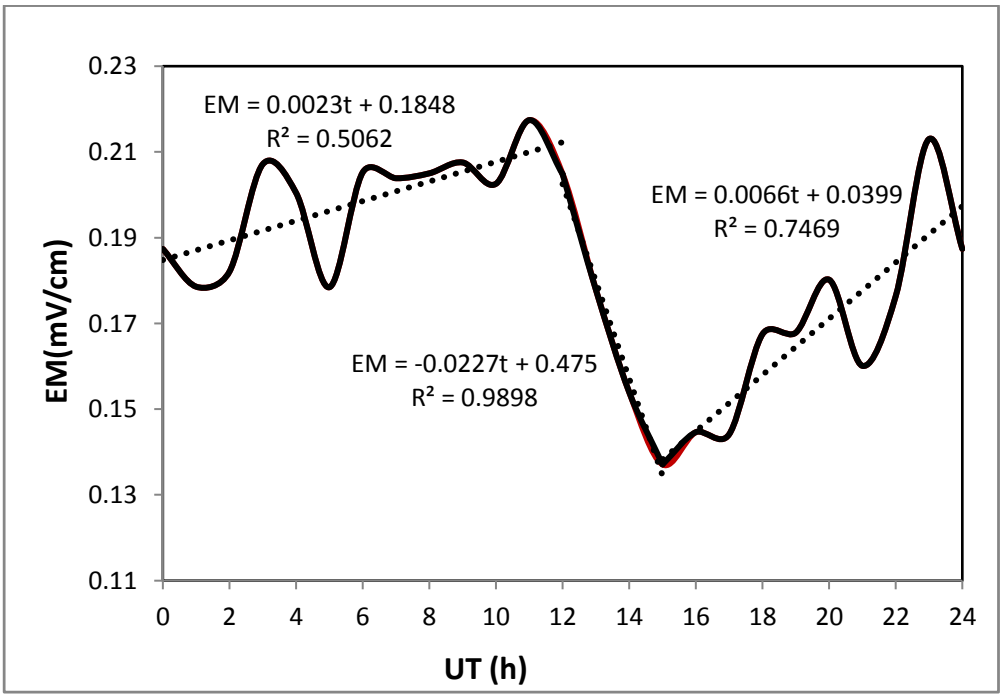

Figure 5. The same as figure 3 but for the all shock activity.

phases per day for the state of the magnetosphere. The first one corresponds to the period of change of the IMF from the northward to the southward and this direction is maintained until 1200 UT. The second phase begins by the change of the IMF from southward to northward and maintains this direction until 1400 UT. The third phase highlights the period of the reconnection at night time.

The comparison between the beginning time of the different phase of the state of the magnetosphere shows that it is better to target each type of disturbed activity instead of investigating the different disturbed activities as a whole disturbed activity.

Figure 6 concerns the MCEF diurnal variation for one-day-shock activity. During this activity, the MCEF exhibits four trends. It emerges from this figure that the MCEF increases from 0000 UT to 1200 UT. The trend slope and the correlation values are $\frac{6.5\ 10^{-3}mV}{cm.s}$ and 0.86, respectively. Between 1200 UT and 1500 UT the MCEF decreases with the trend slope value of - $\frac{2.7\ 10^{-2}mV}{cm.s}$ and the correlation coefficient value of 0.9173. From 1500 UT to 1900 UT we have an increasing phase with the trend slope and the correlation values of $\frac{2.7\ 10^{-2}mV}{cm.s}$ and 0.9173, respectively. After this increase, the MCEF decreases from 1500 UT to 2400 UT. The trend slope for this phase is - $\frac{6.8\ 10^{-3}mV}{cm.s}$ with the correlation coefficient of 0.7495.

The MCEF of the one-day-shock activity varies from the minimum (0.038 mV/cm) to the maximum (0.168 mV/cm) with a mean value of 0.132 mV/cm.

The MCEF of the one-day-shock activity presents four phases: two increasing phases and two decreasing phases. Each increasing phase is followed by a decreasing phase. This let us assert that the IMF turns four times when it acts on the one-day-shock. The latest phase of the overall shock activity corresponds to southward IMF (Figure 5) and that of the one-day-shock shows the signature of the northward IMF (Figure 6).

Analysis of the Figure 6 shows that there is no night side reconnection because the MCEF end the day by its decreasing phase. This is an important result because on one hand, one-day-shock activity impact differs from that of the whole shock activity and on the other hand, the night side reconnection does not occur at all time after the disrobed period.

Figure 7 highlights the time variation of the MCEF during the action of the two-days-shock. From 0000 UT to 1000 UT, the MCEF is fairly constant where its values oscillated between 0.26 mV/cm and 0.225 mV/cm. Between 1000 UT and 1600 UT, the MCEF shows decreasing phase with a slope of - $\frac{1.36\ 10^{-2}mV}{cm.s}$ with the correlation coefficient value of 0.9458. After that, we see an increasing phase from 1600 UT to 2400 UT. The slope of this phase is - $\frac{1.31\ 10^{-2}mV}{cm.s}$ with 0.8788 as correlation coefficient value.

The mean value of the MCEF is 0.229 mV/cm with the minimum value of 0.158 mV/cm and the maximum value of 0.281 mV/cm.

During two-days-shock activity, the magnetosphere

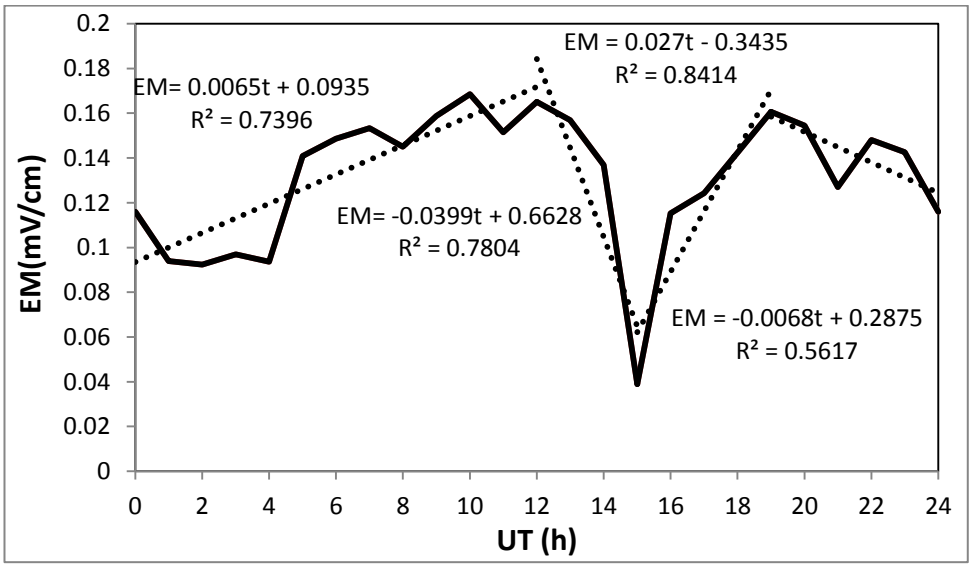

Figure 6. Magnetosphere convection electric field time variation for the one-day-shock activity.

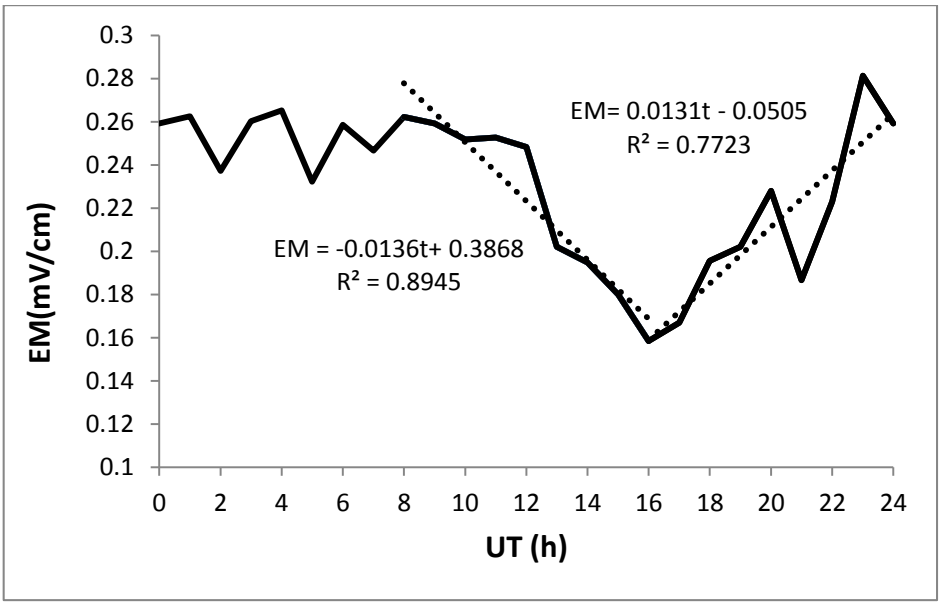

Figure 7. The same as figure 6 but for the two–days-shock activity.

seems to be non-sensitive to this type of shock until 1000 LT by exhibiting a fairly constant trend. The careful analysis of the graph points out that there are shortly successive time-changes (one hour) where the IMF turns from southward (increasing phase of the MCEF) to northward (decreasing phase of the MCEF). After that constant trend, the MCEF presents two trends. The decreasing phase of the MCEF following by the increasing one expresses that the IMF turns from northward to southward. Comparing the action of the one-day-shock and that of the two-days-shock, this remark reveals that added to the difference between the initial phase, another difference is observed during the last phase, the MECF of the one-day-shock activity is northward while that of the two-days-shock activity is southward.

The important conclusion that can be underlined is that it is impossible during two-days-shock period to assert that there is or not night side reconnection.

Figure 8 presents the diurnal variation of the MCEF

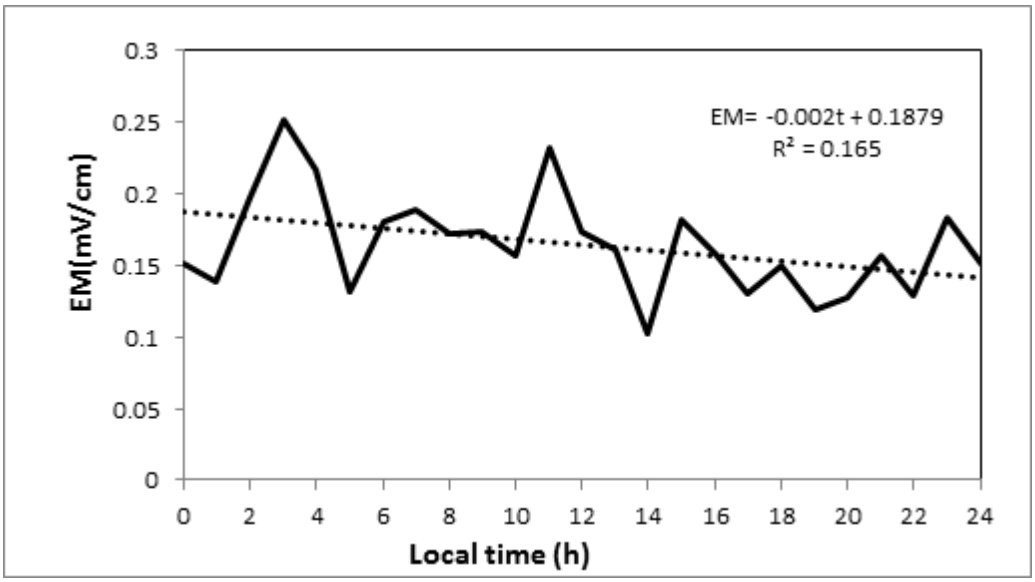

Figure 8. The same as figure 6 but for the three–days-shock activity.

during the three-days-shock activity. One can see the decreasing trend of the MCEF with a slope $-\frac{2\,10^{-3}mV}{cm.s}$ and 0.4062 as correlation coefficient value. The MCEF oscillates between its minimum value (0.101 mV/cm) and its maximum value (0.250 mV/cm) with a mean value of 0.250 mV/cm.

This type of shock is characteristic. In fact, the MCEF time variation shows the trend that characterizes a constant northward IMF due to the decreasing trend of the MCEF. But a careful analysis of the time profile of the MCEF during the three-days-shock activity shows that the IMF is always northward for the first and the last phases. We can assert here that there is no night side reconnection during the period of three-days-shock

Conclusion

The present work shows that the mean amplitudes of the MCEF during the whole disturbed period are inferior to those of the shock activity period. Moreover, during quiet time, the MCEF time profile presents a trough at 1400 LT and for the disturbed period at the same time we observe its maximum value.

It can be retained from this study that for the shock activity, the highest amplitudes of the MCEF are observed during the action of the two-days shock. The amplitudes vary from 0.158 to 0.281 mV/cm with a daily mean value of 0.229 mV/cm. The lowest amplitudes of the MCEF are produced by the one-day shock activity.

Whatever the type of shock, the MCEF intensity decreases from 1200 UT to 1400 UT and also between 2300 UT and 2400 UT. The trough is seen in the profile of the MCEF time variation between 1300 UT and 1700 UT during the shock activity where the minimums occur at 14 00 UT for the three-days-shock activity, at 1600 UT for the two-days-shock activity and at 1500 UT for the overall shock activity and for the one-day-shock activity.

The MCEF time profile during the whole disturbed activity and for the overall shock activity presents three trends (increasing, decreasing and increasing trends) beginning and ending by the southward IMF. The MCEF time profile of the one-day-shock shows four trends beginning by the southward IMF and ending by the northward IMF. The MCEF time profile of the two-days-shock is characterized by the non-sensitive change of the IMF followed by the signature of the northward IMF and finishing by that of the southward IMF. The MCEF of the three-days-shock is continuously decreased. This situation expresses the signature of the northward IMF.

It can be retained that: (1) it is better to treat separately on one hand each type of disturbed activity and on the other hand each type of shock. (2) the night reconnection does not occur during the one-day-shock and three-days-shock activities. For the whole shock activity and the two-days-shock activity it seems to be impossible to assert that there is or not a night time reconnection

CONFLICT OF INTERESTS

The authors have not declared any conflict of interests.

REFERENCES

Axford WI, Hines CO (1961). A unifying theory of high-latitude geophysical phenomena and geomagnetic storms. Canadian Journal of Physics 39:1433-1464.

de Siqueira PM, de Paula ER, Muella MTAH, Rezende LFC, Abdu MA,

Gonzalez WD (2011). Storm-time total electron contznt and its response to penetration electric fields over South America. Annales Geophysicae 29:1765-17778.
Dungey TW (1961). Interplanetary magnetic field and the auroral zones. Physical Review Letters 6(2):47-48.
Gnabahou DA, Ouattara F. (2012) Ionosphere Variability from 1957 to 1981 at Djibouti Station. European Journal of Scientific Research 73(3):382-390.
Gonzalez WD, Joselyn JA, Kamide Y, Kroehl HW, Rostoker G, Tsurutani BT, Vasyliunas VM. (1994). What is a geomagnetic storm? Journal of Geophysical Research 99(A4):5771-5792.
Kelley MC, Fejer BG, Gonzalez CA (1979). An explanation for anomalous ionospheric electric fields associated with northward turning of the interplanetary magnetic field. Geophysical Research Letters 6:301-304.
Gyébré AMF, Ouattara F, Kaboré S, Zerbo JL. (2015) Time variation of shock activity due to moderate and severe CMEs from 1966 to 1998. British Journal of Science 13(1):1-7.
Gyébré AMF, Gnabahou DA, Ouattara F (2018). The geomagnetic effects of solar activity as measured at Ouagadougou Station. International Journal of Astronomy and Astrophysics 8:178-190.
Legrand JP, Simon PA (1989). Solar Cycle and Geomagnetic Activity: A Review for Geophysicists. Part I. The Contributions to Geomagnetic Activity of Shock Waves and of the Solar Wind. Annals of Geophysics 7:565-578.
Mannucci AJ, Tsurutani BT, Abdu MA, Gonzalez WD, Komjathy A, Echer E, Iijima BA, Crowley G, Anderson D (2008). Superposed epoch analysis of the dayside ionospheric response to four intense geomagnetic storms. Journal of Geophysical Research 113:A00A02, doi:10.1029/2007JA012732
Mayaud PN (1971). A Measurement of Planetary Magnetic Activity Based on Two Antipodal Observatories. Annales Geophysicae 27:67-71.
Mayaud PN (1972). The aa Indices: A 100-Year Series, Characterizing the Magnetic Activity. Journal of Geophysical Research 77:6870-6874. http://dx.doi.org/10.1029/JA077i034p06870
McPherron RL, Weygand JM, Hsu TS (2007). Response of the Earth's magnetosphere to changes in the solar wind. Journal of Atmospheric and Solar-Terrestrial Physics Doi:10.1016/jastp.2007.08.040
Nishimura Y, Kikuchi T, Wygant J, Shinbori A, Ono T, Mtsuoka A, Nagatsuma T, Brautigam D (2009). Response of convection electric fields in the magnetosphere to IMF orientation change. Journal of Geophysical Research Vol. 114. A09206, 1-11. doi:10.1029/2009JA014277
Ouattara F, Amory Mazaudier C (2009) Solar-geomagnetic activity and Aa indices toward a standard classification. Journal of Atmospheric and Solar-Terrestrial Physics 71:1736-1748.
Partamies N, Juusola I, Tanskanen E, Kauristie K, Weygand JM, Ogawa Y (2011). Substorms during different phases. Annales Geophysicae 29:2011-2043.
Revah I, Bauer P (1982). Rapport d'activité du Centre de Recherches en Physique de l'environnement Terrestre et Planétaire, Note technique CRPE/115, 38-40 Rue du Général Leclerc 92131 Issy-Les Moulineaux.
Richardson IG, Cane HV. (2002) Sources of Geomagnetic Activity during Nearly Three Solar Cycles (1972- 2000). Journal of Geophysical Research 107:1187.
Richardson IG, Cliver EW, Cane HV (2000). Sources of Geomagnetic Activity over the Solar Cycle: Relative Importance of Coronal Mass Ejections, High-Speed Streams, and Slow Solar Wind. Journal of Geophysical Research 105:18200-18213. http://dx.doi.org/10.1029/1999JA000400
Russel CT (1979). The control of the magnetopause by the interplanetary magnetic fields. 3-21. In Dynamic of the magnetosphere. Akasofu S-I (ed.) University of Alaska, Geophysical Institute, Elvey CT Building, Fairbanks, Alaska, USA.
Russel CT (2007). The coupling of the solar wind to Earth's magnetosphere. In Space weather - Physics and effects. Volker Bothmer and Loannis A. Daglis (ed.) Springer, Praxis Publishing, Chichester, UK. pp. 103-130.
Simon PA, Legrand JP (1989). Solar Cycle and Geomagnetic Activity: A Review for Geophysicists. Part II. The Solar Sources of Geomagnetic Activity and Their Links with Sunspot Cycle Activity. Annals of Geophysics 7:579-594.
Tommaso A, Mirko P, Antonio V, Paula De M, Fabio L, Vincenzo C, Leonardo P (2016). Identification of the different magnetic field contributions during a geomagnetic storm in magnetospheric and ground observations. Annales Geophysicae 34:1069-1084
Zerbo JL, Ouattara F, Zoundi C, Gyébré AMF (2011). Cycle solaire 23 et activité géomagnétique depuis 1868. Révue CAMES-Série A, 12(2):255-262.